

Implementation of a discrete-time quantum walk with a circulant matrix on a graph by optical polarizing elements

Yusuke Mizutani  and Tomoyuki Horikiri 

Faculty of Engineering Division of Intelligent Systems Engineering, Yokohama National University, Hodogaya, Yokohama 240-8501, Japan

Leo Matsuoka 

Faculty of Engineering, Hiroshima Institute of Technology, Hiroshima 731-5193, Japan

Yusuke Higuchi 

Department of Mathematics, Gakushuin University, Tokyo 171-8588, Japan

Etsuo Segawa 

Graduate School of Environment and Information Sciences, Yokohama National University, Hodogaya, Yokohama 240-8501, Japan



(Received 5 May 2022; accepted 19 July 2022; published 5 August 2022)

In this paper, we introduce a quantum walk whose local scattering at each vertex is denoted by a unitary circulant matrix, namely, the circulant quantum walk. We also introduce another quantum walk induced by the circulant quantum walk, namely, the optical quantum walk, whose underlying graph is a 2-regular directed graph and obtained by blowing up the original graph in some way. We propose a design of an optical circuit which implements the stationary state of the optical quantum walk. We show that if the induced optical quantum walk does not have $+1$ eigenvalue, then the stationary state of the optical quantum walk gives that of the original circulant quantum walk. From this result, we give a useful condition for the setting of the circulant quantum walks which can be implemented by this optical circuit.

DOI: [10.1103/PhysRevA.106.022402](https://doi.org/10.1103/PhysRevA.106.022402)

I. INTRODUCTION

Random walks on finite graphs play key roles for analysis of the electrical network (e.g., Ref. [1]) and cutoff phenomena (e.g., Refs. [2,3]). Quantum walks (QWs) are known as the quantum counterpart of such random walks [4,5]. Although the application of QWs to a quantum search algorithm is one of the more remarkable applications [6–8], we also anticipate that such a quantum version of the application will be developed. It is well-known that irreducible random walks on a finite graph converges to the stationary state in the long time limit. This is very fundamental to such applications of random walks. The convergence to the stationary state of random walks is supported by the fact that all the absolute values of the eigenvalues except ± 1 are strictly smaller than 1 because these eigenvalues converge to 0 by the exponentiation of the time steps. On the other hand, the eigenvalues of QWs live on the unit circle in the complex plane. Thus every eigenvalue having the overlap to the initial state asserts its existence even in the long time limit, in general, since the absolute value of the eigenvalue is the unit. Indeed, in the quantum search algorithm, a high probability at the marked vertices is obtained in an asymptotic periodicity of the time evolution with respect to the sufficiently large number of vertices. This derives from the eigenvalues each of whose eigenspace has a large overlap to the initial state. Then if we miss the optimal timing of the

observation, we may have a very low probability of finding the marked vertex [9].

Thus, it is natural to consider finding a stationary state of a QW as a fixed point of a dynamical system [10,11]. In Refs. [12–14], such a QW model where the dynamics converges to a stationary state is proposed by considering a semi-infinite system. In this model, the boundary of the graph and the initial state are set so the unitary time evolution on the whole space, which includes the outside of the graph, describes that some quantum walkers penetrate as the inflow from the outside of the graph to the boundaries and some quantum walkers go out from the boundaries to the outside of the graph as the outflow at every time step. Then it is mathematically shown the dynamical system based on this QW model converges to a fixed point as a stationary state since the inflow to the graph and outflow to the outside are balanced in the long time limit [12–14]. For example, it is shown that the stationary state of the Szegedy walk induced by a reversible random walk with a constant inflow can be expressed by using the current of an electrical circuit [15].

Then, because discrete-time QW is implemented on one- and two-dimensional lattices (see, for example, Refs. [16–18] and references therein) and also continuous-time QW is implemented on the circulant graph [19], and so on, we attempt to consider an implementation of a discrete-time QW having

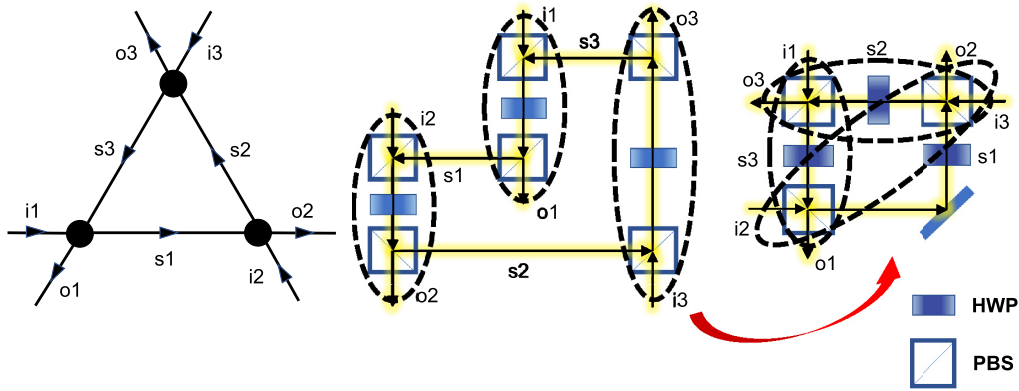


FIG. 1. The island of the blow-up graph (left side), the island mounted with optical elements (middle), and the simplified version of the island mounted with optical elements (right side). This figure corresponds to the islands of $\tilde{G}^{(BU,\xi)}$ for $N = 3$, where each island of $\tilde{G}^{(BU,\xi)}$ is a directed graph with two inputs (i, s) and two outputs (o, s) (for example, on the left, we can see the vertices where i_1 and s_3 are inputs and o_1 and s_1 are outputs). The island on the right is a simplified equivalent of the middle optical island.

the stationary state as a dynamical system on the symmetric digraph induced by a general undirected and connected graph substituting the symmetric arcs into each undirected edge. In Ref. [20], the stationary state of a discrete-time QW model on the one-dimensional lattice gives the stationary Schrödinger equation with delta potentials on \mathbb{R} [21] and a possible approach to the implementation of this QW model using the optical circuit is suggested; the internal graph corresponds to a finite path graph in the setting of our QW treated here. The more detailed mathematical discussion in Ref. [20] from the viewpoint of the spectral and scattering theory can be seen in Ref. [22]. In this paper, based on an idea inspired by Refs. [16,20], in particular, we propose the design of an optical circuit implementing our QW model on a general graph which converges to a stationary state. Moreover, we mathematically find a useful setting of this QW model where the stationary states can be implemented by using this optical circuit, although technical difficulties remain in terms of the implementation. The QW model of our target for the implementation is called the circulant QW. The quantum coin assigned at each vertex, which describes the manner of scattering at each vertex $u \in V$, is given by a $d(u)$ -dimensional circulant matrix. Here $d(u)$ is the degree of the vertex u . The circulant matrix is diagonalized by the discrete Fourier matrix and related to coding theories [23]. The circulant matrix assigned at each vertex coincides with the scattering matrix describing the response of our proposed optical circuit (see Fig. 1).

The main idea of the implementation of the quantum coin is that we embed this local optical circuit into each vertex as the quantum coin and we regard each boundary of the circuit as the gateway leading into one of the adjacent vertices (see Figs. 2, 3, and 4). We heuristically show that this resulting large optical circuit can be represented by the stationary state of another QW model—namely, an optical QW. The underlying graph of the optical QW is a blow-up digraph of the original graph which is two-regular. This two-regularity is represented by horizontal and vertical polarization of the light $|H\rangle$ and $|V\rangle$ in the optical circuit in our proposed very ideal design. To implement the original QW by this optical circuit, the theoretical problem is to clarify the relation between sta-

tionary states of the circulant QW and optical QW. So, if such a stationary state of the circulant QW coincides with that of the optical QW, we say that the optical QW implements the underlying circulant QW. In this paper, we mathematically show a useful sufficient condition for the implementation. The sufficient condition provides a concrete setting of the implementing optical circuit. The setting breaks a kind of symmetricity (see Theorem 2 and Figs. 9 and 10) with respect to the orientation of the circuit or with respect to the quantum coins.

The rest of this paper is organized as follows. In Sec. II, the circulant QW on graph $G = (V, A)$ is introduced. The quantum coin assigned at each vertex is a circulant matrix induced by a two-dimensional unitary matrix H_u . The circulant QW is determined by the sequence $\{H_u\}_{u \in V}$ and labeling

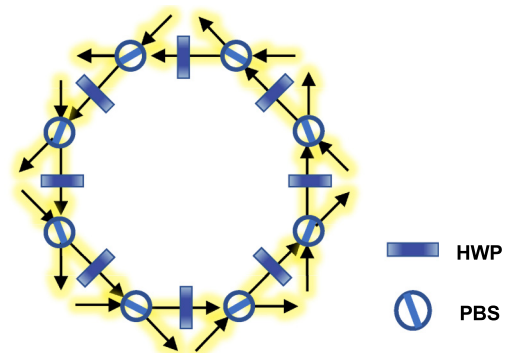


FIG. 2. The island implemented with the optical elements shown on the right of Fig. 1, with N generalized (the figure shown here is for $N = 8$, but it can be extended to general circumscribed polygons). Mirrors are eliminated and the angle of incidence and reflection at the PBS are not taken into account (generally, the angle of incidence and reflection would be 90° , but that is just a matter of changing the direction of the optical path). Each location of HWP corresponds to an individual vertex of the island. Each PBS plays two roles, both receiving the inflows with a superposition of H and V polarizations from the backward HWP and with H polarization from the outside, and sending the outflow with V polarization to the forward HWP and with H polarization to the outside.

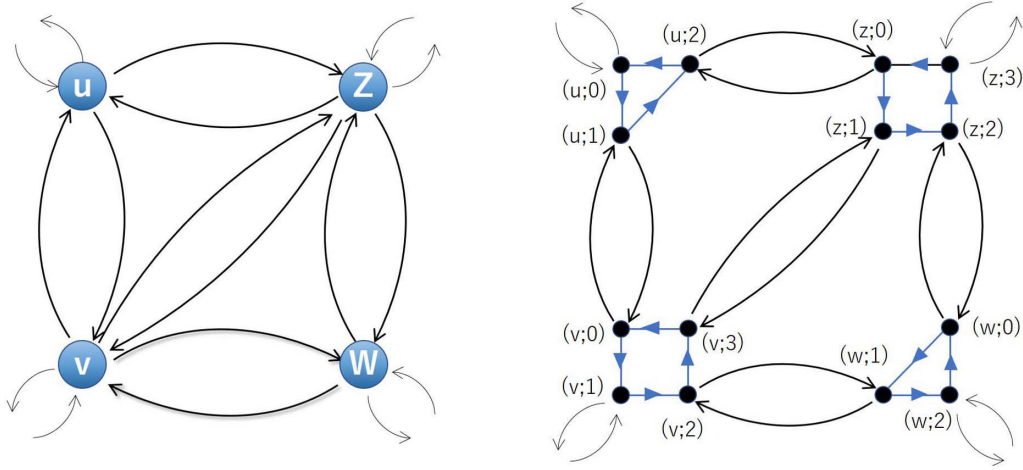


FIG. 3. The original graph G_0 (left) and its blow-up graph $\tilde{G}_0^{(BU,\xi)}$ (right). The labeling ξ is set as follows: $\xi_u(\text{tail}) = 0$, $\xi_u((v, u)) = 1$, $\xi_u((z, u)) = 2$; $\xi_v(\text{tail}) = 1$, $\xi_v((w, v)) = 2$, $\xi_v((z, v)) = 3$, $\xi_v((u, v)) = 0$; $\xi_w(\text{tail}) = 2$, $\xi_w((z, w)) = 0$, $\xi_w((v, w)) = 1$; $\xi_z(\text{tail}) = 3$, $\xi_z((u, z)) = 0$, $\xi_z((v, z)) = 1$, $\xi_z((w, z)) = 2$. For example; (i) there is an arc from $(u; 2)$ to $(u; 0)$ because the terminal vertices are commonly u and $2 + 1 = 0$ in the modulus of $\text{deg}(u) = 3$, which satisfies the connected condition (1) in Definition 3, and (ii) there are symmetric arcs between vertex $(v; 2)$ and $(w; 1)$ in $\tilde{G}_0^{(BU,\xi)}$ because we can check that $\alpha(\xi_v^{-1}(2)) = \alpha((w, v)) = w$ and $\alpha(\xi_w^{-1}(1)) = \alpha((v, w)) = v$, which satisfies the connected condition (2) in Definition 3.

$\{\xi_u\}_{u \in V}$, where $\xi_u : A_u \rightarrow \{0, \dots, \text{deg}(u) - 1\}$ is a bijection map. Here A_u is the set of all the arcs of G whose terminal vertices are $u \in V$. In Sec. III, we introduce the optical QW on the blow-up directed graph induced by the original graph of the circulant graph. Then the optical QW is determined by the same parameters of the circulant QW. Our target is to find a useful condition for the setting of the circulant QW in which the stationary state of the circulant QW can be obtained by referring to that of the optical QW. The motivation for the target derives from the expectation that the optical QW can be implemented by an optical circuit using polarizing

elements proposed by Sec. IV. In particular, the design of the optical circuit is proposed for the circulant QW on an arbitrary connected graph in Sec. IV. In Sec. V, we demonstrate numerically the case for the complete graph with ten vertices, K_{10} . The first example is the case that the implementation works while the second example is the case that the implementation does not work. In Sec. VI, a solution to the concrete labeling way $\{\xi_u\}_{u \in V}$ for the implementation is proposed using a key proposition. The key proposition gives a sufficient condition for the implementation: If the induced optical QW does not have eigenvalue 1, then the implementation

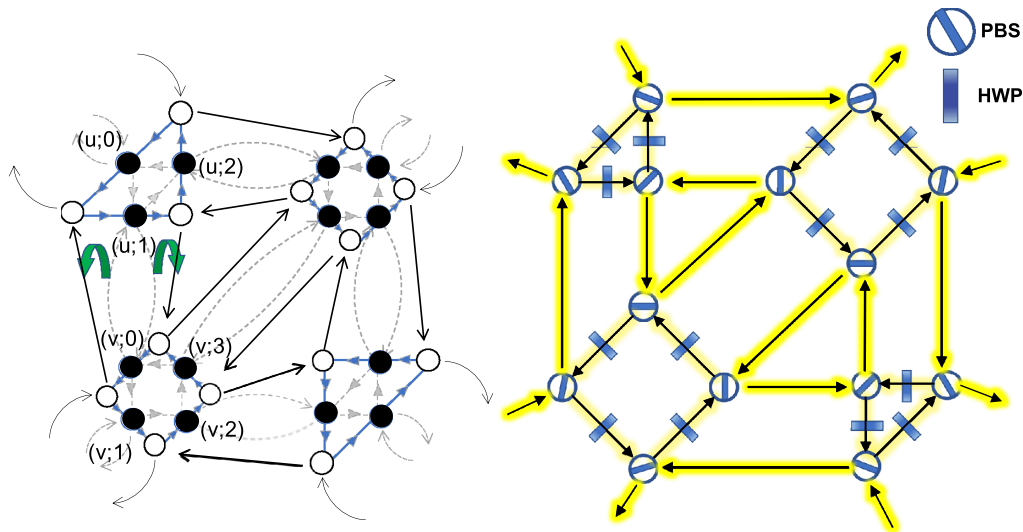


FIG. 4. G' (left) and the design of the optical circuit (right). To highlight the act of drawing the circuit, we include $\tilde{G}_0^{(BU,\xi)}$ in gray on the left. We draw the circumscribed polygons around each island (blue arcs) and place the vertices on the corners and in the midpoint of each side. Then, the sides of the circumscribed polygon correspond to A_0^{cycle} . On the other hand, all the arcs in \tilde{A}_0 are reconnected as depicted on the left. For example, the symmetric arcs between $(u; 1)$ and $(v; 0)$ are reconnected by changing the origin and terminal vertices to the corresponding corners of the circumscribed polygon. We set the half-wave plate on each black vertex and the polarizing beam splitter on each white vertex as depicted on the right.

works. In Sec. VII, we present the useful conditions for the implementation in the complete graph K_N case. In Sec. VIII, we give the proof for the key proposition. Finally, we provide the summary and discussion of our results. The important notations are listed in the last page.

II. CIRCULANT QUANTUM WALK ON GRAPHS

A. Setting of the graph and labeling

Let $G = (V, A)$ be a connected digraph where V is the set of the vertices and A is the set of arcs. If every arc $a \in A$ has the inverse arc $\bar{a} \in A$, we call this graph a symmetric digraph. The terminal and origin vertices of $a \in A$ are denoted by $t(a)$ and $o(a)$, respectively. Let $G_0 = (V_0, A_0)$ be a finite and connected symmetric digraph. To this original graph G_0 , in this paper, we connect the semi-infinite path to *every* vertex. This resulting infinite graph is denoted by $\tilde{G}_0 = (\tilde{V}_0, \tilde{A}_0)$. We set the degree of vertex $u \in V_0$ by

$$\deg(u) := \{a \in \tilde{A}_0 \mid t(a) = u\} = \{a \in \tilde{A}_0 \mid o(a) = u\}.$$

The set of the boundary of G_0 ; ∂A_{\pm} is defined by

$$\begin{aligned} \partial A_+ &= \{t(a) \in V_0, o(a) \notin V_0\}, \\ \partial A_- &= \{o(a) \in V_0, t(a) \notin V_0\}. \end{aligned}$$

In the following, we introduce the concept of the labeling, which plays an important role in describing the time evolution of the QWs treated here. Let $A_u \subset \tilde{A}_0$ be the set of arcs whose terminal vertices are commonly $u \in \tilde{V}_0$; that is, $A_u = \{a \in \tilde{A}_0 \mid t(a) = u\}$.

Definition 1. Labeling of arcs: The labeling of the arcs of $\tilde{G}_0 = (\tilde{V}_0, \tilde{A}_0)$ is defined by the series of the bijection maps $(\xi_u)_{u \in \tilde{V}_0}$. Here ξ_u is a bijection map such that

$$A_u \rightarrow \{0, \dots, \deg(u) - 1\}.$$

Note that the number of choices of the labeling $\xi = (\xi_u)_u$ of \tilde{G}_0 is $\prod_{u \in \tilde{V}_0} \deg(u)!$; we choose a labeling from one of these choices.

B. Circulant quantum walk

In this subsection, we introduce the circulant QW on the infinite graph $\tilde{G}_0 = (\tilde{V}_0, \tilde{A}_0)$ with the labeling $\xi = (\xi_u)_{u \in \tilde{V}_0}$, which has tails defined as described in the previous subsection. For a discrete set Ω , we define \mathbb{C}^Ω as the vector space whose standard basis is described by each element of Ω ; that is, $\mathbb{C}^\Omega = \text{span}\{\delta_\omega \mid \omega \in \Omega\}$. Here δ_ω is

$$\delta_\omega(\omega') = \begin{cases} 1 & : \omega = \omega' \\ 0 & : \omega \neq \omega'. \end{cases}$$

For a two-dimensional unitary matrix assigned at each vertex $u \in V_0$,

$$H_u = \begin{bmatrix} a_u & b_u \\ c_u & d_u \end{bmatrix},$$

we introduce the following $\deg(u) \times \deg(u)$ -circulant matrix $\text{Circ}(H_u)$ induced by the 2×2 -matrix H_u , such that $[\text{Circ}(H_u)]_{i,j=0}^{\deg(u)-1} = w_{i-j}^{(u)}$, where $i - j$ is the modulus of

$\deg(u)$; that is,

$$\text{Circ}(H_u) = \begin{bmatrix} w_0^{(u)} & w_{\deg(u)-1}^{(u)} & w_{\deg(u)-2}^{(u)} & \cdots & w_1^{(u)} \\ w_1^{(u)} & w_0^{(u)} & w_{\deg(u)-1}^{(u)} & \cdots & w_2^{(u)} \\ w_2^{(u)} & w_1^{(u)} & w_0^{(u)} & \cdots & w_3^{(u)} \\ \vdots & \ddots & \ddots & \ddots & \vdots \\ w_{\deg(u)-1}^{(u)} & w_{\deg(u)-2}^{(u)} & w_{\deg(u)-3}^{(u)} & \cdots & w_0^{(u)} \end{bmatrix}. \quad (1)$$

Here $w_\ell^{(u)}$ is defined by

$$\begin{aligned} w_0^{(u)} &= d_u + \frac{b_u c_u}{1 - a_u^\kappa} a_u^{\kappa-1}, \\ w_\ell^{(u)} &= \frac{b_u c_u}{1 - a_u^\kappa} a_u^{\ell-1} \quad (\ell = 1, \dots, \kappa - 1). \end{aligned}$$

Throughout this paper, we assume $a_u b_u c_u d_u \neq 0$ to avoid a trivial dynamics of the QW.

Assumption 1. For any $u \in V_0$, we assume $a_u b_u c_u d_u \neq 0$.

The $\deg(u) \times \deg(u)$ matrix; $\text{Circ}(H_u)$, is a unitary matrix; see Lemma 3 for more details.

To explain exactly how the QW iterates the time evolution on the graph \tilde{G}_0 with the labeling ξ driven by the circulant matrix, let us introduce $\chi_u : \mathbb{C}^{\tilde{A}} \rightarrow \mathbb{C}^{[\deg(u)]}$ by the restriction to $\mathbb{C}^{[\deg(u)]}$ such that $(\chi_u \psi)(a) = \psi(\xi_u(a))$. The adjoint operator is described by

$$(\chi_u^* f)(a) = \begin{cases} f(\xi^{-1}(a)) & : a \in A_u \\ 0 & : a \notin A_u. \end{cases}$$

A matrix representation of the map χ_u is expressed by the $\deg(u) \times \infty$ matrix,

$$\chi_u \cong [I_{\deg(u)} \mid 0],$$

under the decomposition of the set of arcs into $A_u \sqcup (\tilde{A} \setminus A_u)$. Now we are ready to give the definition of the circulant QW on graph \tilde{G} with the labeling ξ .

Definition 2. Circulant QW on \tilde{G}_0 : $QW(G_0; \{H_u\}_{u \in V_0}; \{\xi_u\}_{u \in \tilde{V}_0})$

- (i) The total vector space: $\mathbb{C}^{\tilde{A}_0}$
- (ii) The time evolution operator:

$$\tilde{U}_0 = U(G_0; \{H_u\}_{u \in V_0}; \{\xi_u\}_{u \in \tilde{V}_0}) = SC.$$

Here S is the flip flop shift operator such that $(S\psi)(a) = \psi(\bar{a})$ for any $\psi \in \mathbb{C}^{\tilde{A}}$, $a \in \tilde{A}$, and C is defined by

$$C = \bigoplus_{u \in \tilde{V}} \chi_u^* C_u \chi_u$$

under the decomposition of $\mathbb{C}^{\tilde{A}_0} = \bigoplus_{u \in \tilde{V}_0} \mathbb{C}^{A_u}$, where

$$C_u = \begin{cases} \text{Circ}(H_u) & : u \in V_0 \\ \sigma_X & : u \notin V_0, \end{cases}$$

and σ_X is the Pauli matrix.

(iii) The initial state:

$$\psi_0(a) = \begin{cases} 1 & : a \notin A_0, \text{dist}(o(a), V_0) > \text{dist}(t(a), V_0) \\ 0 & : \text{otherwise.} \end{cases}$$

We call this QW the circulant QW on G_0 .

It is possible to extend this initial state, for example, by setting the inflow to each vertex represented by $\alpha \in \mathbb{C}^V$ such that

$$\psi_0(a) = \begin{cases} \alpha(u) & : a \in A(\mathbb{P}_u) (u \in V_0), \\ & \text{dist}(o(a), V_0) > \text{dist}(t(a), V_0) \\ 0 & : \text{otherwise.} \end{cases}$$

Here $A(\mathbb{P}_u)$ is the set of arcs of the tail connected to vertex $u \in V_0$. The QW with such an initial state also converges to a stationary state [12–14]. In this paper, we fix the initial state as the uniform for simplicity.

Let us explain the important points of the time iteration of this QW. Let ψ_n be the n th iteration by $\psi_{n+1} = \tilde{U}_0 \psi_n$. The dynamics on the tails is free such that if the arcs of a tail are labeled by a_0, a_1, a_2, \dots with $o(a_0) \in V_0, t(a_j) = o(a_{j+1})$ ($j = 0, 1, 2, \dots$), then

$$\begin{bmatrix} \psi_{n+1}(a_{j+1}) \\ \psi_{n+1}(\bar{a}_j) \end{bmatrix} = \sigma_X \begin{bmatrix} \psi_n(\bar{a}_{j+1}) \\ \psi_n(a_j) \end{bmatrix} = \begin{bmatrix} \psi_n(a_j) \\ \psi_n(\bar{a}_{j+1}) \end{bmatrix}. \quad (2)$$

This means that a quantum walker is perfectly transmitting at each vertex on the tails. Note that the free QW on the tails is independent of the labeling of the vertices. On the other hand, the QW in the internal graph depends on the labeling. At each vertex on the internal graph G_0 , a quantum walker is scattered by $\text{Circ}(H_u)$ as follows:

$$\begin{aligned} & \begin{bmatrix} \psi_{n+1}(\overline{\xi_u^{-1}(0)}) \\ \vdots \\ \psi_{n+1}(\overline{\xi_u^{-1}(\text{deg}(u) - 1)}) \end{bmatrix} \\ &= \text{Circ}(H_u) \begin{bmatrix} \psi_n(\xi_u^{-1}(0)) \\ \vdots \\ \psi_n(\xi_u^{-1}(\text{deg}(u) - 1)) \end{bmatrix} \end{aligned} \quad (3)$$

for any $u \in V_0$. The initial state ψ_0 is set so $\psi_n(a) = \psi_0(a)$ for any $n \geq 0$ and $a \in \partial A_+$. Therefore, a quantum walker is provided to the internal graph G_0 as the inflow from ∂A_+ while a quantum walker is consumed as the outflow to ∂A_- at every time step.

III. OPTICAL QUANTUM WALK ON THE BLOW-UP GRAPHS

In this section, we introduce another QW on the blow-up graph induced by $\tilde{G}_0 = (\tilde{V}_0, \tilde{A}_0)$ with the labeling ξ . This QW is called the optical QW. As we will see, the optical QW is implemented by a circuit of the optical polarizing elements in theory. Moreover, the stationary state of the optical quantum walk coincides with that of the circulant quantum walk under some conditions.

To explain the implementation design and the condition in greater detail, let us first introduce the definitions of the blow-up graph and the optical quantum walk precisely.

A. Blow-up graph

Let $\tilde{G}_0 = (\tilde{V}_0, \tilde{A}_0)$ be the original graph with the tails. Recall that the bijection map $\xi_u : A_u \rightarrow [\text{deg}(u)] := \{0, \dots, \text{deg}(u) - 1\}$ is assigned at each vertex u as defined by the previous section. The labeling is denoted by $\xi := (\xi_u)_{u \in \tilde{V}_0}$. Under this setting, the blow-up graph of \tilde{G}_0 is defined as follows. See also Fig. 3.

Definition 3. Blow-up graph of \tilde{G}_0 with the labeling $\xi : \tilde{G}_0^{(\text{BU}, \xi)} = (\tilde{V}_0^{(\text{BU}, \xi)}, \tilde{A}_0^{(\text{BU}, \xi)})$.

The vertex and arc sets are defined as follows:

$$\tilde{V}_0^{(\text{BU}, \xi)} = V_0^{(\text{BU})} \cup (\tilde{V}_0 \setminus V_0), \quad (4)$$

$$\tilde{A}_0^{(\text{BU}, \xi)} = A_0^{(\text{BU}, \xi)} \cup (\tilde{A}_0 \setminus A_0). \quad (5)$$

Here

$$V_0^{(\text{BU})} := \sqcup_{u \in V_0} \{(u; \xi_u(a)) \mid t(a) = u\}$$

and $A_0^{(\text{BU}, \xi)}$ is defined as follows. There is an arc from $(u; j) \in V_0^{(\text{BU}, \xi)}$ to $(v; \ell) \in V_0^{(\text{BU}, \xi)}$ in $\tilde{G}_0^{(\text{BU}, \xi)}$; that is, $((u; j), (v; \ell)) \in A_0^{(\text{BU}, \xi)}$, if and only if either of the following two conditions hold:

- (i) $u = v$ and $\ell = j + 1$ in the modulus of $\text{deg}(u)$ or
- (ii) $v = o(\xi_u^{-1}(j))$ and $u = o(\xi_v^{-1}(\ell))$ in \tilde{G}_0 .

Each tail connecting to vertex $u \in V_0$ in the original graph \tilde{G}_0 is connected to the vertex $(u; \xi_u(a))$ with $a \in \partial A_+$ in the blow-up graph $\tilde{G}_0^{(\text{BU}, \xi)}$.

The blow-up graph is constructed by (i) blowing up each vertex $u \in V(G_0)$ as the *directed cycle* following the labeling ξ_u and by (ii) connecting to other oriented cycles by the symmetric arcs following the original connection in G_0 . Then, if vertices u and v are connected in G_0 , there are symmetric arcs between the directed cycle of u obtained by (i) and that of v in \tilde{G}_0 . We call the directed cycle of u in the new graph $\tilde{G}_0^{(\text{BU}, \xi)}$ obtained by (i) the *island* of u . The set of all the arcs in all the islands is denoted by A_0^{cycle} , which is the set of arcs of the oriented cycles by the blowing up. On the other hand, since the arcs obtained by (ii) in Definition 3 are isomorphic to \tilde{A}_0 , we denote this set by \tilde{A}_0 itself to reduce the number of notations.

Remark 1. The set of arcs $\tilde{A}_0^{(\text{BU}, \xi)}$ is divided into

$$\tilde{A}_0^{(\text{BU}, \xi)} = A_0^{\text{cycle}} \sqcup \tilde{A}_0.$$

The blow-up graph is not a symmetric-directed graph; that is, the existence of the inverse arc is not ensured and it has more vertices and arcs than the original graph, which would seem to suggest a complexity. On the other hand, it has the following nice property.

Remark 2. The blow-up graph is a 2-regular digraph; that is, for every vertex $u \in \tilde{V}_0^{(\text{BU}, \xi)}$, the in degree and the out degree are two; one pair of in arc and out arc belongs to A_0^{cycle} and the other belongs to \tilde{A}_0 .

The reason for replacing the original vertex u in \tilde{G}_0 with island u in $\tilde{G}_0^{(\text{BU}, \xi)}$ is to represent the two polarizations of the optics as follows. A quantum optics is driven by two polarizations represented by $|V\rangle = [1, 0]^T$ and $|H\rangle = [0, 1]^T$. Instead of such a complexity of the blowing up graph, we obtain a representation of the two internal degrees of freedom

on every vertex in the blow-up graph because of the two-regularity. The subset \tilde{A}_0 keeps the fundamental structure of the original graph. This fact will play an important role in the implementation of the circulant QW on graph \tilde{G}_0 by a quantum optics.

B. Optical quantum walk and the motivation

The time evolution operator of the optical QW is determined by the parameters of the previous circulant QW. The graph of the optical QW is the blow-up graph $\tilde{G}_0^{(\text{BU}, \xi)}$. Recall that the in and out degrees of the blow-up graph are two. The vector space of the time evolution is represented by $\mathbb{C}^{\tilde{A}_0^{(\text{BU}, \xi)}}$. The scattering at each vertex (u, j) is expressed by H_u . More precisely, we define the optical QW as follows.

Definition 4. Optical QW on $\tilde{G}_0^{(\text{BU}, \xi)}$: $\text{Opt}(\text{QW}(\tilde{G}_0; \mathbf{H}; \xi))$.

(i) The vector space: $\mathbb{C}^{\tilde{A}_0^{(\text{BU}, \xi)}}$.

(ii) The time evolution: Let $a_{\text{in}} \in A_0^{\text{cycle}}$, $b_{\text{in}} \in \tilde{A}_0$ be the arcs whose terminal vertices are (u, j) , and $a_{\text{out}} \in A_0^{\text{cycle}}$, $b_{\text{out}} \in \tilde{A}_0$ be the arcs whose origins are also (u, j) . Then the time evolution operator $U^{(\text{BU})}$ is defined as follows:

$$\begin{bmatrix} (U^{(\text{BU})}\psi)(a_{\text{out}}) \\ (U^{(\text{BU})}\psi)(b_{\text{out}}) \end{bmatrix} = H_u \begin{bmatrix} \psi(a_{\text{in}}) \\ \psi(b_{\text{in}}) \end{bmatrix} \quad (6)$$

for any $\psi \in \mathbb{C}^{\tilde{A}_0^{(\text{BU}, \xi)}}$. On the tails, the dynamics of the QW is free; that is, it follows (2).

(iii) The initial state:

$$\psi_0(a) = \begin{cases} 1 & : a \notin A_0^{(\text{BU}, \xi)}, \\ & : \text{dist}(o(a), V_0^{(\text{BU})}) > \text{dist}(t(a), V_0^{(\text{BU})}) \\ 0 & : \text{otherwise.} \end{cases}$$

Our interest is how the optical QW imitates the original circulant QW. One of them can be implemented by a quantum optics in theory. An experimental implementation of $\psi_\infty^{(\text{BU})}$ by optical polarizing elements is proposed in Sec. IV. According to Ref. [14], both of the stationary states for the circulant QW and its induced optical QW exist:

Theorem 1 ([14]). Let ψ_n and $\psi_n^{(\text{BU})}$ be the n th iterations of the circulant QW and its induced optical QW. Then we have

$$\exists \lim_{n \rightarrow \infty} \psi_n =: \psi_\infty, \quad \exists \lim_{n \rightarrow \infty} \psi_n^{(\text{BU})} =: \psi_\infty^{(\text{BU})}.$$

We can then focus on their stationary states and the condition for the two stationary states to coincide.

Definition 5. Notion of the implementation in this paper : We say that the optical QW implements the underlying circulant QW if

$$\psi_\infty^{(\text{BU})}(a) = \psi_\infty(a) \text{ for any } a \in \tilde{A}_0.$$

In Sec. V, we give examples by numerical simulation.

IV. A CIRCUIT OF OPTICAL POLARIZING ELEMENTS FOR THE OPTICAL QUANTUM WALK

In this section, we propose the design of the optical circuit implementing the optical QW in an ideal environment where the phase is matched in each interference and there is no attenuation. Improvement points for a more realistic design are discussed in the final section.

First, we introduce our idea for the implementation of the island in $\tilde{G}_0^{(\text{BU}, \xi)}$ by using the half wave plate (HWP) and polarizing beam splitter (PBS) so the output to arbitrary input of this optical circuit is represented by our circulant matrix. Second, we explain how to connect each implemented circuit to reproduce the dynamics on the optical QW.

A. Design of $U^{(\text{BU})}|_{\text{island } u}$

In this subsection, we design the parts of the circuit for the optical QW which will be placed on the islands in the blow-up graph. The island u is represented by a directed cycle with the tails. Let \tilde{C}_N be such a directed graph with N vertices. See Fig. 1 for the $N = 3$ case. We introduce an implementation of the QW restricted to the island \tilde{C}_N driven by 2×2 matrix H by optical polarizing elements. Let us explain the implementation by the following three steps.

1. Direct implementation ($N = 3$).

First, let us focus on the implementation for the $N = 3$ case. The stationary state of the QW on the left side of Fig. 1, \tilde{C}_3 , is described as

$$\begin{bmatrix} s_k \\ o_k \end{bmatrix} = H \begin{bmatrix} s_{k-1} \\ i_k \end{bmatrix} \quad (7)$$

for any $k = 0, 1, 2$. The middle of Fig. 1 depicts a direct implementation approach in which the dynamics of the QW on the island is mounted with optical elements. Each HWP in the middle figure is sandwiched between two PBSs (surrounded by dotted lines), which corresponds to one of the vertices of \tilde{C}_3 . There are two modes of polarization, H polarization and V polarization. The fundamental idea of our implementation is that we establish a correspondence between the arcs of \tilde{C}_3 and the modes of polarization; that is, each arc of the triangle in the left part of the figure corresponds to the V polarization while each arc of the tail in the left part of the figure corresponds to the H polarization. Since PBS is responsible for transmitting an H polarization and reflecting a V polarization, the first PBS in the vertex k ($k = 1, 2, 3$) represents the situation that the vertex k receives the inflow of quantum walkers from both inside (s_{k-1}) and outside (i_k) while the second PBS represents the situation that the vertex k sends the outflow to both inside (s_k) and outside (o_k). We have set the inflow vectors $[s_{k-1} \ i_k]^T$ and outflow vectors $[s_k \ o_k]^T$ ($k = 1, 2, 3$) in (7). With PBS alone, there is no factor that can affect the polarization state. Then we set the HWP between the two PBSs, which shifts the phase of each polarization; as a consequence, input H polarization results in a superposition of the H and V polarizations. Thus, the sandwiched HWP represents the unitary operator H in (7). In summary, the sandwiched HWP plays the role of the operation of quantum coin H , while the first and second PBSs play the role of giving the inflow of a quantum walker to vertex k represented by $[s_{k-1} \ i_k]^T$ and the outflow of a quantum walker from the vertex k represented by $[s_k \ o_k]^T$ in (7), respectively.

Note that it is possible to make an arbitrary unitary matrix H by setting additional quarter-wave plates [24]. More precisely, arbitrary two-dimensional unitary matrix H can be

represented by

$$H = e^{i\delta/2} \exp(-\frac{1}{2}i\xi\sigma_2) \exp(\frac{1}{2}i\eta\sigma_3) \exp(-\frac{1}{2}i\zeta\sigma_2),$$

with some real-valued four parameters δ, ξ, η, ζ . Such unitary matrix can be implemented by two quarter-wave plates and one HWP such that

$$H = e^{i\delta/2} \tilde{Q}\left[\frac{\xi}{2} + \frac{\pi}{4}\right] \tilde{H}\left[\frac{\xi + \eta - \zeta}{4} - \frac{\pi}{4}\right] \tilde{Q}\left[-\frac{\zeta}{4} + \frac{\pi}{4}\right], \quad (8)$$

[24], for example. Here $\tilde{H}[\theta]$ (respectively, $\tilde{Q}[\theta]$) corresponds to the half- (respectively, quarter-) wave plate with slow axis at θ angle, respectively, that is,

$$\tilde{H}[\theta] = C[\theta, \pi], \quad \tilde{Q}[\theta] = C[\theta, \pi/2],$$

with

$$C[\theta, \eta] := e^{-i\theta\sigma_2} \begin{bmatrix} e^{i\eta/2} & 0 \\ 0 & e^{-i\eta/2} \end{bmatrix} e^{i\theta\sigma_2}.$$

The phase shifter $e^{i\delta/2}$ is implemented by adjusting the optical path length in the circuit, for example. Throughout this paper, HWP denotes the set of two quarter-wave plates, one HWP, and the phase shifter represented by (8), which implements the unitary matrix H . Also note that there are fixed-end and free-end reflections in PBSs. In the situation we are considering here, the V polarization only appears on s_k , corresponding to the vertex k of the island. Therefore, at i_k and o_k , where V polarization does not need to be taken into account, there is no reflection at the PBS and the phase π is not affected by the fixed end. For these reasons, the island shown on the right of Fig. 1 should be mounted so the fixed-end faces the outside of the island.

2. Economical implementation ($N = 3$)

In the second step, to reduce the optical elements, we introduce an economical design as depicted on the right of Fig. 1. Let us explain that we can omit the route between the first PBS in the forward vertex and the second PBS in the backward vertex in the middle of Fig. 1, which means that we combine the PBS for the inflow placed in vertex k with the PBS for the outflow placed in vertex $k - 1$ ($k = 0, 1, 2$). In the middle of Fig. 1, let us focus on the optical route denoted by the arc from the HWP to the second PBS placed in vertex 3. Let us denote the state on this arc by w_3 . This state w_3 is described by a superposition of polarizations H and V. The outflow o_3 corresponds to the V polarization while s_3 corresponds to the H polarization. The state s_3 will be reflected on the first PBS placed in vertex 1. Then the state between the first PBS and HWP placed in vertex 1 is described by $s_3 + i_1$. Next, let us focus on the corresponding optical route between the HWP and the combined PBS on the right side of Fig. 1. The state before the combined PBS on the right is w_3 and the state after the combined PBS is split into $s_3 + i_1$ as the inflow to vertex 1 and o_3 as the outflow from vertex 3. Then the response to the inflows on the left of the figure is isomorphic to that of the middle. Note that the in- and outflows on each PBS derive from the different vertices in this implementation.

3. Extension to $N \geq 3$

As a third step, the idea for $N = 3$ can be extended to a general $N \geq 3$. In Fig. 2, we draw the resulting design for general N . The island with the vertices N ; \tilde{C}_N , can be considered in the same way as the right of Fig. 1. Each location of the HWP corresponds to each vertex of the island. Each PBS takes both roles, receiving the inputs from the backward vertex and from the outside, and sending the outputs to the forward vertex and to the outside. Then, the input from the outside corresponds to a quantum walker from the outside to the *forward* vertex, while the output to the outside corresponds to a quantum walker from the outside from the *backward* vertex. This means that at each PBS, the vertex of the output to the outside shifts that of the input from the outside by one. This observation will be important to design the whole circuit.

B. Drawing the circuit

We build the circuit by combining the above parts (islands). We introduce the method drawing the circuit so each outflow from an island is switched to another inflow to a neighboring island. In the following, the blow-up graph $\tilde{G}_0^{(BU, \xi)}$ is deformed to $G' = (\text{HWP} \sqcup \text{PBS}, A')$ to draw the circuit. After drawing graph G' , we place the HWP on each HWP vertex in the island u and the PBSs on each PBS vertex in G' . Now let us explain how to draw graph G' from the blow-up graph $\tilde{G}_0^{(BU, \xi)}$.

1. Vertex set

We begin by drawing the circumscribed polygon to each original island in $\tilde{G}_0^{(BU, \xi)}$. The vertex set of G' is constructed by all the corners of the circumscribed polygons and all the sides of the circumscribed polygons. The vertex subset on the corners is denoted by PBS, while the vertex subset on the sides is denoted by HWP. The HWP vertex is in one-to-one correspondence with the vertex set of the original graph $\tilde{G}_0^{BU, \xi}$.

2. Arc set

Following the orientation of each island, the sides of the circumscribed polygon with the subdivision by HWP vertices are replaced with the arcs in G' . Next, let us define the remaining arcs in G' . Let us set the arc from the islands u to v in $\tilde{G}_0^{(BU, \xi)}$ by $a \in \tilde{A}_0$. The origin and terminal vertices of a in $\tilde{G}_0^{(BU, \xi)}$ are denoted by $(u; \xi_u(v))$ and $(v; \xi_v(u))$, respectively.¹ In G' , the arc a is replaced with the arc whose origin vertex is the PBS vertex located in the corner between $(u; \xi_u(v))$ and $(u; \xi_u(v) + 1)$ and the terminus vertex is the PBS vertex located in the corner between $(v; \xi_v(u))$ and $(v; \xi_v(u) - 1)$. The same reconnection procedure is done to every arc in \tilde{A}_0 . Then the new graph G' is obtained.

The reason for the reconnection procedure is as follows. From the consideration of the economical design in Sec. IV A

¹Originally, the domain of ξ_u was the arc set whose terminal vertices are u in \tilde{G}_0 , but since there is a one-to-one correspondence between the above arcs and their origin vertices if G_0 is a simple graph, we change the domain to the vertex set for readability.

(see also Fig. 2), we know that the PBS vertex between the HWP vertex $(u; \xi_u(v))$ and $(u; \xi_u(v) + 1)$ must play the two roles, receiving inflow from the islands $\xi_u^{-1}(\xi_u(v) + 1)$ and sending outflow to the island v . It is implied that the forward PBS vertex of the HWP vertex located at $(u; \xi_u(v))$ sends the outflow to the island v while the backward PBS vertex of the HWP vertex located in $(u; \xi_u(v) - 1)$ receives the inflow from the island v . By switching the situation of the islands from u to v , we see that the forward PBS vertex sends the outflow to island u while the backward vertex receives the inflow from island u . Thus, in the optical circuit graph G' , the arc from $(u; \xi_u(v))$ to $(v; \xi_v(u))$ in $\tilde{G}_0^{(\text{BU}, \xi)}$ must be replaced with the arc from the PBS vertex between the HWP vertices $\xi_u(v)$ and $\xi_u(v) + 1$ to the PBS vertex between the HWP vertices $\xi_v(v) - 1$ and $\xi_v(u)$ in the optical design graph G' . Then we realize the situation that each outflow from an island is switched to another inflow to a neighboring island by using the designs of $U^{(\text{BU})}_{\text{island } u}$'s. A more realistic implementation and arising problems will be discussed in the final section.

V. DEMONSTRATION BY NUMERICAL SIMULATIONS

In this section, we examine whether a circulant QW on the complete graph with ten vertices, K_{10} , is implemented by the corresponding optical QW by changing H . The arc whose terminus is i and origin is j is denoted by (i, j) , and the arc whose terminus is i and origin is located in the tail is denoted by (i, i) in \tilde{G}_0 . The labeling $\xi = (\xi_0, \dots, \xi_9)$ is given as follows:

$$\xi_i((i, j)) = j \tag{9}$$

for every $i, j = 0, \dots, 9$. We consider the following two examples. First, we consider the case in which the implementation is realized, and then we consider the case where the implementation fails. For this purpose, we define a relative

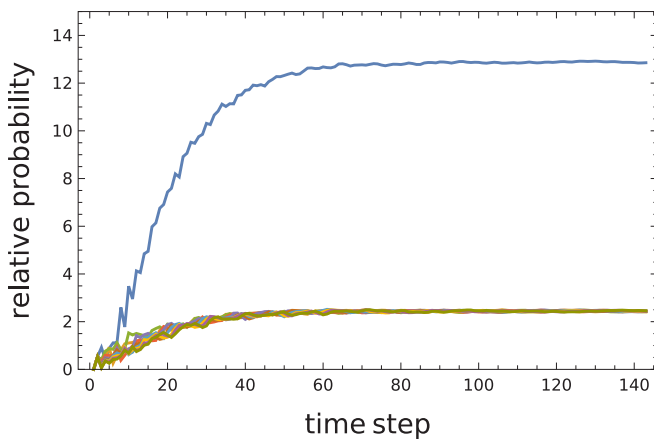


FIG. 5. Time course of μ_n for the circulant QW with a marked vertex in the setting of Example 1: The horizontal and vertical lines are the time step and the relative probability of each vertex. The blue (upper) line is the time course of the relative probability of the marked vertex, the other lines are the time courses of the other vertices.

probability of the circulant QW by

$$\mu_n(j) = \sum_{a \in \tilde{A}_0: t(a)=j} |\psi_n(a)|^2.$$

We also set

$$\mu_n^{\text{BU}}(j) = \sum_{a \in \tilde{A}_0: t(a)=j} |\psi_n^{\text{BU}}(a)|^2,$$

and chase their time courses μ_n and μ_n^{BU} simultaneously. Note that the summation is taken over \tilde{A}_0 in the definition of $\mu_n^{(\text{BU})}$ because the implementation is determined at the original arcs of G_0 by Definition 5. The existence of limits of $n \rightarrow \infty$ to μ_n and μ_n^{BU} is ensured by Theorem 1. We call $\lim_{n \rightarrow \infty} \mu_n$ a stationary measure of the circulant QW.

Example 1. K_{10} with a marked vertex: We choose the vertex 0 in the set of vertices $\{0, \dots, 9\}$ as the marked vertex. The circulant coin assigned at each vertex is denoted by $\text{Circ}(H_j)$. Here H_j is set so a perturbation is given only at the marked element 0 as follows:

$$H_j = \begin{cases} \begin{bmatrix} 1/\sqrt{2} & 1/\sqrt{2} \\ 1/\sqrt{2} & -1/\sqrt{2} \end{bmatrix} & : j = 0 \\ \begin{bmatrix} 1/\sqrt{2} & 1/\sqrt{2} \\ -1/\sqrt{2} & 1/\sqrt{2} \end{bmatrix} & : \text{otherwise} \end{cases}$$

for $j = 0, \dots, 9$. The unitary matrix H_0 can be implemented by setting $\xi = -\zeta = 2 \arccos \sqrt{p}$, $\eta = -\pi$ and $\delta = \pi$ as the parameters of the half- and quarter-wave plates and the phase shifter, respectively, in (8), while the unitary matrix H_j for $(j \neq 0)$ can be implemented by setting $\xi = \zeta = -\theta$, $\eta = 0$ and $\delta = 0$. Here $p := (1 + 1/\sqrt{2})/2$. Figure 5 shows the time course of the relative probability at each vertex $0, \dots, 9$. The blue (upper) curve describes the time course of the relative probability of vertex 0, which is the marked vertex. We observe that although the timescales of the convergence are different, the stationary measures converge to the same value for every vertex in Fig. 6. This is theoretically supported by Theorem 2

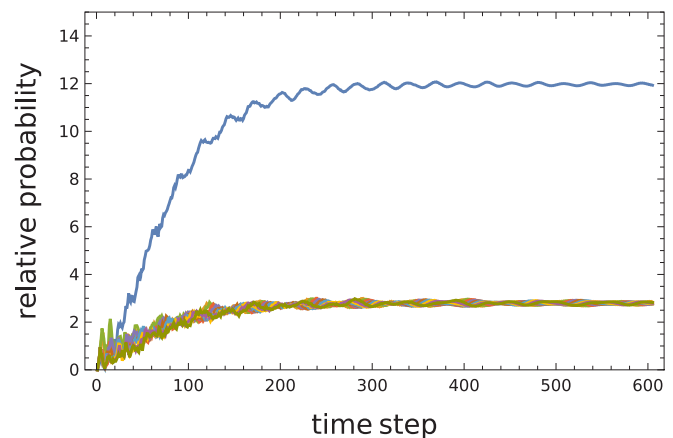


FIG. 6. Time course of μ_n^{BU} for the optical QW with a marked vertex induced by the left circulant QW: The blue (upper) line is the time course of the relative probability of the marked vertex, the other lines are the time courses of the other vertices.

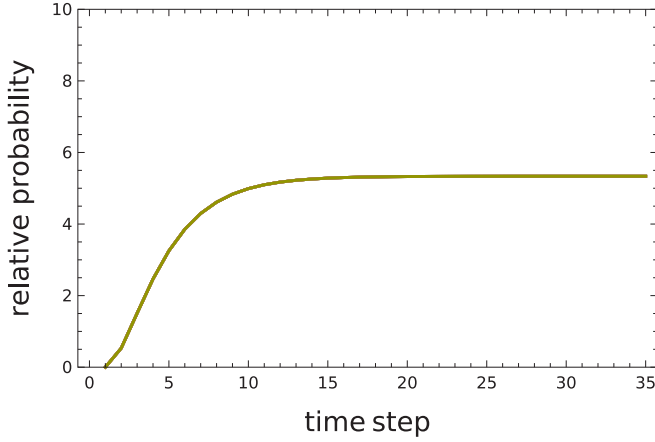


FIG. 7. Time course of the relative probabilities of the uniform circulant QW in the setting of Example 2.

because there are arcs in $G_0^{(\text{BU};\xi)}$ satisfying condition (ii) in the corollary; these arcs are (0,1) and (0,9) and their inverses.

Example 2. (K_{10} with the uniform setting) We assign H_j 's uniformly by

$$H_j = \begin{bmatrix} 1/\sqrt{2} & 1/\sqrt{2} \\ 1/\sqrt{2} & -1/\sqrt{2} \end{bmatrix}$$

for any $j = 0, \dots, 9$. From the symmetry on the time evolution with respect to each vertex, the stationary measure on each vertex is the same. In Figs. 7 and 8, we observe that although both the circulant QW and its induced optical QW converge to some stationary measures, the convergence values are different.

VI. MATHEMATICAL RESULTS

The following sufficient condition for the accomplishment of the implementation is the key to our main results:

Proposition 1. Let $\mathbf{H} = (H_u)_{u \in V_0}$ and $\xi = (\xi_u)_{u \in V}$ in the setting of the circulant quantum walk $\text{QW}(G_0; \mathbf{H}; \xi)$ on \tilde{G}_0 . If $\ker(1 - U^{(\text{BU})}) = \{\mathbf{0}\}$, then $\text{Opt}(\text{QW}(G_0; \mathbf{H}; \xi))$ on $\tilde{G}_0^{(\text{BU};\xi)}$ implements $\text{QW}(G_0; \mathbf{H}; \xi)$ on \tilde{G}_0 .

Proof. See Sec. VIII. \blacksquare

The following theorem gives a sufficient condition for $\ker(1 - U^{(\text{BU})}) = \{\mathbf{0}\}$, which illustrates two kinds of the setting of the optical QW. See Figs. 9 and 10; a kind of symmetry is broken around the boundary because (i) the rotational orientations of the connected islands are opposite each other or (ii) the assigned coins of the connected islands are different.

Theorem 2. (The symmetry-breaking designs for the implementation.)

Assume that

$$H_u = \begin{bmatrix} a_u & b_u \\ c_u & d_u \end{bmatrix}$$

satisfies $a_u b_u c_u d_u \neq 0$ for any $u \in V_0$. If there is an arc $e \in A_0$ satisfying each of them:

- (i) $\xi_{o(e)}(\bar{e}) - \xi_{o(e)}(e) = \xi_{t(e)}(e) - \xi_{t(e)}(\tau) = \pm 1$ or
- (ii) $\xi_{o(e)}(\bar{e}) - \xi_{o(e)}(e) = -(\xi_{t(e)}(e) - \xi_{t(e)}(\tau)) = \pm 1$ and $d_{o(e)} \neq d_{t(e)}^*$,

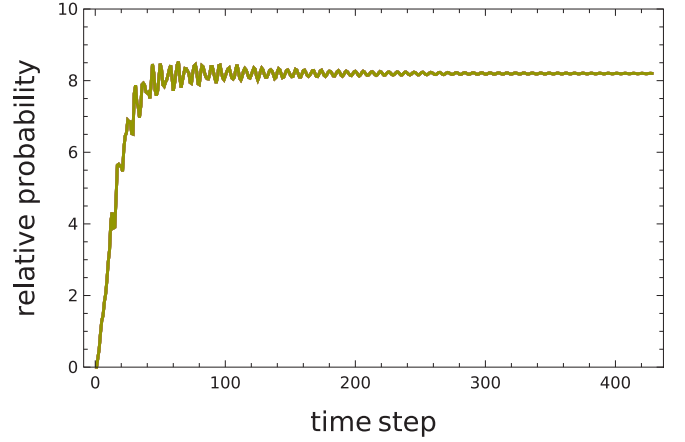


FIG. 8. Time course of the relative probabilities of the uniform optical QW induced by the left circulant QW.

where $t, \tau \in \partial A_+$ whose terminal vertices are located in the islands $o(e)$ and $t(e)$, respectively, then $\text{Opt}(\text{QW}(G_0; \mathbf{H}; \xi))$ implements $\text{QW}(G_0; \mathbf{H}; \xi)$. Here for a complex number z , z^* is the conjugate of z .

Example 1 in Sec. V matches the setting of case (ii) in Theorem 2. This is the reason that the stationary state of the circulant QW coincides with that of its optical QW. Now we give the proof using Proposition 1.

Proof. The arc in ∂A_+ whose terminal vertex is $u \in V_0$ is denoted by τ_u . We set $B_u \subset A_0^{(\text{BU};\xi)}$ as the set of arcs whose terminal or origin vertices are $(u, \xi_u(\tau_u))$ (see Fig. 11):

$$B_u = \{a \in A_0^{(\text{BU};\xi)} \mid o(a) = (u, \xi_u(\tau_u)) \text{ or } t(a) = (u, \xi_u(\tau_u))\}.$$

The eigenvector of eigenvalue 1 is denoted by ψ . Note that ψ satisfies not only $U^{(\text{BU};\xi)}\psi = \psi$ but also $\|\psi\|^2 < \infty$. First, let us see if the following fact holds:

$$\text{supp}(\psi) \cap (\cup_{u \in V_0} B_u) = \emptyset. \quad (10)$$

In the tail, $\psi(\tau_u) = \psi(a_1) = \psi(a_2) = \dots$ and $\psi(\bar{\tau}_u) = \psi(\bar{a}_1) = \psi(\bar{a}_2) = \dots$ (where $o(\tau_u) = t(a_1)$, $o(a_1) = t(a_2), \dots$) holds. Then to ensure $\|\psi\| < \infty$, the values $\psi(\tau_u)$ and $\psi(\bar{\tau}_u)$ must be 0. From the definition of the time evolution operator of this QW, letting $e'_{\text{in}}, e'_{\text{out}} \in B_u$, we have

$$\begin{bmatrix} \psi(e'_{\text{out}}) \\ \psi(\bar{\tau}_u) \end{bmatrix} = \begin{bmatrix} a_u & b_u \\ c_u & d_u \end{bmatrix} \begin{bmatrix} \psi(e'_{\text{in}}) \\ \psi(\tau_u) \end{bmatrix},$$

which is equivalent to

$$\begin{aligned} \psi(\tau_u) &= (\psi(e'_{\text{out}}) - a_u \psi(e'_{\text{in}})) b_u^{-1}, \\ \psi(\bar{\tau}_u) &= c_u \psi(e'_{\text{in}}) + (\psi(e'_{\text{out}}) - a_u \psi(e'_{\text{in}})) b_u^{-1} d_u. \end{aligned}$$

This implies that $\psi(\tau_u), \psi(\bar{\tau}_u) = 0$ if and only if $\psi(e'_{\text{out}}), \psi(e'_{\text{in}}) = 0$. Then (10) holds.

Considering the contraposition of Proposition 1, we notice that it is enough to show that if $\ker(1 - U^{(\text{BU})}) \neq \{\mathbf{0}\}$, then there are no arcs in A_0 satisfying (i) or (ii). For $a \in A_0$, let

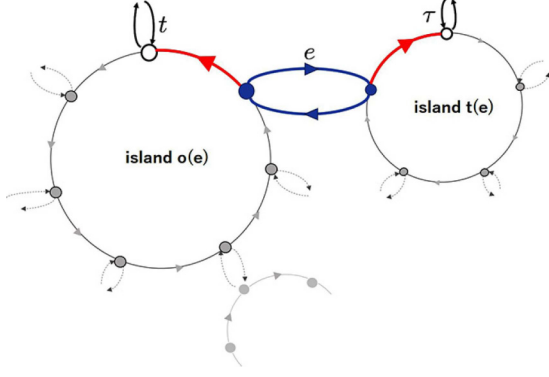


FIG. 9. The symmetry breaking design in Theorem 2 (i) for the implementation.

us put $e_1, e_2 \in A^{\text{cycle}}$ with $t(e_1) = (o(a); \xi_{o(a)}(\bar{a}))$ and $t(e_2) = (t(a); \xi_{t(a)}(a))$ (see Fig. 11). Assume (i) holds, and consider the +1 case. By (10), we have

$$\begin{bmatrix} 0 \\ \psi(a) \end{bmatrix} = \begin{bmatrix} a_{o(a)} & b_{o(a)} \\ c_{o(a)} & d_{o(a)} \end{bmatrix} \begin{bmatrix} \psi(e_1) \\ \psi(\bar{a}) \end{bmatrix},$$

$$\begin{bmatrix} 0 \\ \psi(\bar{a}) \end{bmatrix} = \begin{bmatrix} a_{t(a)} & b_{t(a)} \\ c_{t(a)} & d_{t(a)} \end{bmatrix} \begin{bmatrix} \psi(e_2) \\ \psi(a) \end{bmatrix}.$$

From the unitarity of $H_{o(a)}$ and $H_{t(a)}$, we have $\psi(a), \psi(\bar{a}) \neq 0$. Taking the inverses of $H_{o(a)}$ and $H_{t(a)}$ to both equations, which are the adjoints of them, we also have $\psi(\bar{a}) = d_{o(a)}^* \psi(a)$ and $\psi(a) = d_{t(a)}^* \psi(\bar{a})$. This implies $|d_{o(a)} d_{t(a)}| = 1$. The unitarity of H_u 's leads to $|d_{o(a)}| = |d_{t(a)}| = 1$, which induces $b_u = c_u = 0$ ($u \in \{o(a), t(a)\}$). This is the contradiction to Assumption 1. In the same way, the case for -1 in (i) can be proved. In the next, let us assume (ii) holds. Consider +1 case. Then we have

$$\begin{bmatrix} 0 \\ \psi(a) \end{bmatrix} = \begin{bmatrix} a_{o(a)} & b_{o(a)} \\ c_{o(a)} & d_{o(a)} \end{bmatrix} \begin{bmatrix} \psi(e_1) \\ \psi(\bar{a}) \end{bmatrix},$$

$$\begin{bmatrix} \psi(\bar{e}_2) \\ \psi(\bar{a}) \end{bmatrix} = \begin{bmatrix} a_{t(a)} & b_{t(a)} \\ c_{t(a)} & d_{t(a)} \end{bmatrix} \begin{bmatrix} 0 \\ \psi(a) \end{bmatrix}.$$

Taking the inverse, which is the adjoint of $H_{o(a)}$, to the first equation, we have $d_{o(a)}^* \psi(a) = \psi(\bar{a})$, while computing the second equation directly, we have $\psi(\bar{a}) = d_{t(a)} \psi(a)$; which implies $\psi(\bar{a})/\psi(a) = d_{o(a)}^* = d_{t(a)}$. The -1 case also can be done in the same way. ■

VII. THE CONDITIONS OF $\ker(1 - U^{\text{BU}}) = 0$ FOR K_N CASE

In this section, let us consider the optical QW induced by the circulant QW with the uniform circulant coin on the complete graph with N vertices K_N ; $\text{QW}(K_N; \mathbf{H}; \xi)$. Here the labeling $\xi = (\xi_i)_{i=0}^{N-1}$ is the same as in (9) and the unitary matrices $\mathbf{H} = (H_i)_{i=0}^{N-1}$ are denoted by

$$H_i = H = \begin{bmatrix} a & b \\ c & d \end{bmatrix},$$

with $abcd \neq 0$. In this setting, we obtain a useful sufficient condition to the parameters a, b, c, d of the circulant QW for the implementation as follows.

Theorem 3. Let the circulant QW on K_N be set as described in the above. If $d \notin \mathbb{R}$ or $\det(H)^{2N} \neq 1$ for

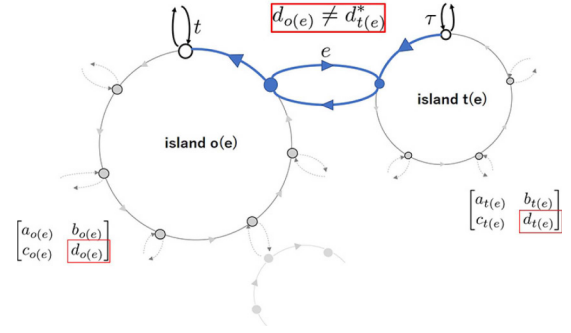


FIG. 10. The symmetry-breaking design in Theorem 2 (ii) for the implementation.

($N > 3$), $\det(H)^{2N} \neq -1$ for ($N = 3$), then the induced optical QW implements the circulant QW.

In the setting of Example 2, the above condition is not satisfied because $\det(H) = -1$ ($a = b = c = -d = 1/\sqrt{2}$). Now let us move to the proof.

Proof. Let us first prepare the following key lemma for the proof.

Lemma 1. Let $N \geq 3$ and $\Delta := \det(H)$. We have

$\dim \ker(1 - U^{\text{BU}})$

$$= \begin{cases} N/2 - 1 & : d \in \mathbb{R}, (-\Delta)^{2N} = 1, N \text{ is even} \\ (N-3)/2 & : d \in \mathbb{R}, (-\Delta)^{2N} = 1, (-\Delta)^N \neq 1, N \text{ is odd} \\ (N-1)/2 & : d \in \mathbb{R}, (-\Delta)^N = 1, N \text{ is odd} \\ 0 & : \text{otherwise.} \end{cases}$$

By Lemma 1, if $d \notin \mathbb{R}$ or $\Delta^{2N} \neq 1$, Theorem 1 implies that the optical QW implements the underlying circulant QW. ■

Now we focus on the proof of Lemma 1.

Proof of Lemma 1. Assume $\ker(1 - U^{\text{BU}}) = 0$. The labeling ξ satisfies with condition (ii) in Theorem 2. Then with the (2,2) element of H ; d must be a real number. Let $U^{\text{BU}}\Psi = \Psi$ and $\text{supp}(\Psi)$ be included in the internal blow-up graph. Each vertex in $\tilde{G}_0^{\text{BU}, \xi}$ is labeled by (ℓ, m) . Here ℓ represents the island and m represents the island heading from the island ℓ . The arc whose origin is (ℓ, m) and terminus is $(\ell, m+1)$ belongs to A_0^{cycle} , where $m+1$ is the modulus of N , while the arc whose origin and terminus are $(\ell, m), (m, \ell)$, respectively,

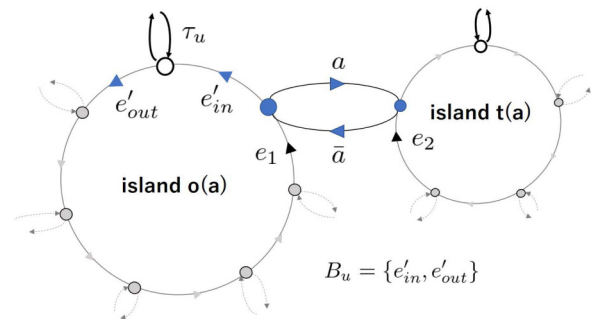


FIG. 11. The vertex colored white is the vertex connecting to a tail. The eigenvector of eigenvalue 1 does not overlap to B_u , for any island u .

belongs to \tilde{A}_0 . We define (ℓ, ℓ) as the vertex connecting to the tail. We also define $((\ell, \ell), (\ell, \ell))$ as the arc from (ℓ, ℓ) to the tail. We set

$$\Psi((\ell, m-1), (\ell, m)) =: z_m^{(\ell)}, \quad \text{and} \quad \Psi((\ell, m), (m, \ell)) =: x_{\ell, m}.$$

Note that since the support of Ψ is included in the internal graph, $x_{\ell, \ell} = 0$ for any $\ell = 0, \dots, N-1$. All the indexes of z and x are the modulus of N . Then we have the following useful lemma.

Lemma 2. We have

$$\begin{bmatrix} x_{\ell, m} \\ x_{m, \ell} \end{bmatrix} = \frac{1}{b} \begin{bmatrix} d & 1 \\ 1 & d \end{bmatrix} \begin{bmatrix} z_{m+1}^{(\ell)} \\ -\Delta z_m^{(\ell)} \end{bmatrix}, \quad (11)$$

$$\begin{bmatrix} z_{m+1}^{(\ell)} \\ -\Delta z_m^{(\ell)} \end{bmatrix} = \sigma_X \begin{bmatrix} z_{\ell+1}^{(m)} \\ -\Delta z_\ell^{(m)} \end{bmatrix} \quad (12)$$

for any $\ell, m = 0, \dots, N-1$.

Proof. By inserting the time evolution of the optical QW in Definition 4 into the eigenequation $U^{\text{BU}}\Psi = \Psi$, we have

$$\begin{aligned} \begin{bmatrix} z_{m+1}^{(\ell)} \\ x_{\ell, m} \end{bmatrix} &= \begin{bmatrix} a & b \\ c & d \end{bmatrix} \begin{bmatrix} z_m^{(\ell)} \\ x_{m, \ell} \end{bmatrix}, \\ \begin{bmatrix} z_{\ell+1}^{(m)} \\ x_{m, \ell} \end{bmatrix} &= \begin{bmatrix} a & b \\ c & d \end{bmatrix} \begin{bmatrix} z_\ell^{(m)} \\ x_{\ell, m} \end{bmatrix}. \end{aligned} \quad (13)$$

Solving $x_{\ell, m}$ and $x_{m, \ell}$ from each equation, we obtain

$$\begin{aligned} \begin{bmatrix} x_{\ell, m} \\ x_{m, \ell} \end{bmatrix} &= \frac{1}{b} \begin{bmatrix} d & -\Delta \\ 1 & -\Delta d \end{bmatrix} \begin{bmatrix} z_{m+1}^{(\ell)} \\ z_m^{(\ell)} \end{bmatrix}, \\ \begin{bmatrix} x_{m, \ell} \\ x_{\ell, m} \end{bmatrix} &= \frac{1}{b} \begin{bmatrix} d & -\Delta \\ 1 & -\Delta d \end{bmatrix} \begin{bmatrix} z_{\ell+1}^{(m)} \\ z_\ell^{(m)} \end{bmatrix}. \end{aligned} \quad (14)$$

Here we used $a = \Delta \bar{d} = \Delta d$ which derives from the unitarity of H and Theorem 2. Then putting $z_m^{(\ell)} := [z_{m+1}^{(\ell)}, z_m^{(\ell)}]^\top$, we have

$$\begin{aligned} \frac{1}{b} \begin{bmatrix} d & -\Delta \\ 1 & -\Delta d \end{bmatrix} z_m^{(\ell)} &= \sigma_X \frac{1}{b} \begin{bmatrix} d & -\Delta \\ 1 & -\Delta d \end{bmatrix} z_\ell^{(m)} \\ \Leftrightarrow \begin{bmatrix} d & 1 \\ 1 & d \end{bmatrix} \begin{bmatrix} 1 & 0 \\ 0 & -\Delta \end{bmatrix} z_m^{(\ell)} &= \sigma_X \begin{bmatrix} d & 1 \\ 1 & d \end{bmatrix} \begin{bmatrix} 1 & 0 \\ 0 & -\Delta \end{bmatrix} z_\ell^{(m)} \\ \Leftrightarrow \begin{bmatrix} 1 & 0 \\ 0 & -\Delta \end{bmatrix} z_m^{(\ell)} &= \begin{bmatrix} d & 1 \\ 1 & d \end{bmatrix}^{-1} \sigma_X \begin{bmatrix} d & 1 \\ 1 & d \end{bmatrix} \begin{bmatrix} 1 & 0 \\ 0 & -\Delta \end{bmatrix} z_\ell^{(m)} \\ \Leftrightarrow \begin{bmatrix} 1 & 0 \\ 0 & -\Delta \end{bmatrix} z_m^{(\ell)} &= \sigma_X \begin{bmatrix} 1 & 0 \\ 0 & -\Delta \end{bmatrix} z_\ell^{(m)}. \end{aligned}$$

Here we used

$$\begin{bmatrix} 1 & d \\ d & 1 \end{bmatrix} \sigma_X = \sigma_X \begin{bmatrix} 1 & d \\ d & 1 \end{bmatrix}$$

in the last equivalence. \blacksquare

From this lemma, we obtain two observations.

Observation 1.

Inserting $\ell = m$ in (14), we have $z_{\ell+1}^{(\ell)} = z_\ell^{(\ell)} = 0$ since $x_{\ell, \ell} = 0$. This is consistent with Theorem 2 in the case of (ii).

Observation 2.

Since ℓ, m are arbitrarily chosen from $0, \dots, N-1$, Eq. (12) is equivalent to $z_m^{(\ell)} = (-\Delta) z_\ell^{(m-1)}$ for any $\ell, m =$

$0, \dots, N-1$. Starting from this, we recursively obtain

$$\begin{aligned} z_m^{(\ell)} &= (-\Delta) z_\ell^{(m-1)} = (-\Delta)^2 z_{m-1}^{(\ell-1)} \\ &= (-\Delta)^3 z_{\ell-1}^{(m-2)} = (-\Delta)^4 z_{m-2}^{(\ell-2)} \\ &= \dots \\ &= (-\Delta)^{2N-1} z_{\ell-N+1}^{(m-N)} = (-\Delta)^{2N} z_{m-N}^{(\ell-N)} = (-\Delta)^{2N} z_m^{(\ell)}. \end{aligned} \quad (15)$$

Then we have $(-\Delta)^{2N} = 1$ or $z_m^{(\ell)} = 0$. If $(-\Delta)^{2N} = 0$, then $z_m^{(\ell)} = 0$ for all ℓ, m and (12) implies $x_{\ell, m} = 0$ for all ℓ, m . This is contradiction. Thus, at least $(\Delta)^{2N} = 1$ must be satisfied.

In the set of pairs of superscript and subscript $[i, j] \in \{[\ell - k, m - k] \mid k = 0, \dots, N\}$ of z in the third column of the above equations, the pair $[\ell, m]$ first appears again as $[m - N, \ell - N]$; on the other hand, in the second column, there might be a $k < N$ such that $[\ell - k, m - k - 1] = [m, \ell]$ in the modulus of N . But such a k can be identified with $k = \ell - m = (N - 1)/2$. Thus, if such an appearance of k happens, the size N must be odd and the arc of $z_m^{(\ell)}$ is located in the front of the vertex (ℓ, ℓ) . In particular, if $N = 3$, since $z_{\ell+1}^{(\ell)} = z_\ell^{(\ell)}$, by the observation 1, every arc in the support of Ψ living in A_0^{cycle} is located in the front of the vertex (ℓ, ℓ) ($\ell = 0, 1, 2$). Therefore, $(-\Delta)^{2k+1} = (-\Delta)^N$ must be 1 for $N = 3$. If $N > 3$ and N is even, the length of such a cycle is $2N$ from (15). This means that we obtain the eigenvector which is constructed by the orbit of $2N$ -length closed path starting from the arc of $z_m^{(\ell)}$ and returning back to this arc. The number of arcs in $A_0^{(\text{cycle})}$ is N^2 , but Observation 1 implies the $2N$ arcs are eliminated as the support of Ψ . Then we have $(N^2 - 2N)/(2N) = N/2 - 1$ linearly independent eigenvectors of eigenvalue 1; that is, $\dim \ker(1 - U^{\text{BU}}) = N/2 - 1$ if $N > 3$ is even, and $(\Delta)^{2N} = 1$. On the other hand, if $N > 3$ and $\ell - m \neq (N - 2)/2$, then the length of the orbit of the closed path represented by (15) is $2N$. Then, if $N > 3$ is odd and $(-\Delta)^{2N} = 1$ but $(-\Delta)^N \neq 1$, we have $(N^2 - (2N + N))/(2N)$ linearly independent eigenvectors of eigenvalue 1; while $N > 3$ is odd and $(-\Delta)^N = 1$, we have $(N^2 - (2N + N))/(2N) + 1$ linearly independent eigenvectors of eigenvalue 1. We have completed the proof of Lemma 1. \blacksquare

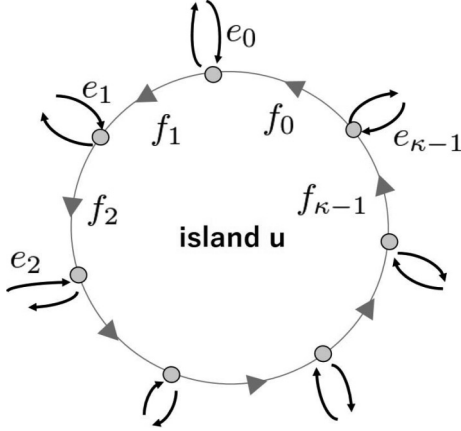
VIII. PROOF OF KEY STATEMENT (PROPOSITION 1)

Let us consider the stationary state of the optical QW ψ^{BU} that satisfies $U^{\text{BU}}\psi^{\text{BU}} = \psi^{\text{BU}}$. The arcs of the island u in $\tilde{G}_0^{\text{BU}, \xi}$ are denoted by

$$\begin{aligned} A_{0,u}^{\text{cycle}} &:= \{a \in A_0^{\text{cycle}} \mid t(a) = u \text{ in } \tilde{G}_0\} \\ &= \{f_0, \dots, f_{\deg_{\tilde{G}_0}(u)-1}\} \subset \tilde{A}_0^{\text{BU}, \xi}. \end{aligned}$$

Here we set $t(f_j) = (u, j)$ in $\tilde{G}_0^{\text{BU}, \xi}$ for $j = 0, \dots, \deg_{\tilde{G}_0}(u)$ (see Fig. 12). The restriction to the island u is defined by $\eta_u : \mathbb{C}^{\tilde{A}_0^{\text{BU}, \xi}} \rightarrow \mathbb{C}^{A_{0,u}^{\text{cycle}}}$ such that $(\eta_u \psi)(a) = \psi(a)$ for any $a \in A_{0,u}^{\text{cycle}}$ and $\psi \in \mathbb{C}^{\tilde{A}_0^{\text{BU}, \xi}}$; the adjoint is

$$(\eta_u^* f)(a) = \begin{cases} f(a) & : a \in A_{0,u}^{\text{cycle}} \\ 0 & : \text{otherwise.} \end{cases}$$

FIG. 12. Labeling of the arcs of island u in the proof of Lemma 3.

Note that $\eta_u \eta_u^*$ is the identity operator on $\mathbb{C}^{A_0^{\text{cycle}}}$ while $\eta_u^* \eta_u$ is the projection operator. Then we have

$$\begin{aligned} U^{\text{BU}} \psi^{\text{BU}} &= \psi^{\text{BU}} \\ \Rightarrow \eta_u U^{\text{BU}} \psi^{\text{BU}} &= \eta_u \psi^{\text{BU}} \\ \Leftrightarrow \eta_u U^{\text{BU}} (\eta_u^* \eta_u + (1 - \eta_u^* \eta_u)) \psi^{\text{BU}} &= \eta_u \psi^{\text{BU}} \\ \Leftrightarrow E_u \varphi_{u,0} + \rho_u &= \varphi_{u,0}, \end{aligned}$$

where $E_u := \eta_u U^{\text{BU}} \eta_u^*$, $\varphi_{u,0} := \eta_u \psi^{\text{BU}}$, and $\rho_u := \eta_u U^{\text{BU}} (1 - \eta_u^* \eta_u) \psi^{\text{BU}}$. Let P_u be the cyclic permutation matrix on $\mathbb{C}^{[\kappa]}$ such that $(P_u \phi)(j) = \phi(j+1)$ in the modulus of $\kappa = \deg_{\tilde{G}_0}(u)$. Then it is easy to see that E_u is isomorphic to $a_u P_u$. Since $|a_u| < 1$, the inverse matrix of $(1 - E_u)$ exists. Then we have

$$\varphi_{u,0} = (1 - E_u)^{-1} \rho_u, \quad (16)$$

where if we label the $\kappa := \deg_{\tilde{G}_0}(u)$ arcs from the outside of island u whose terminal vertices in $\tilde{G}_0^{\text{BU},\xi}$ are $(u; 0), (u; 1), \dots, (u; \kappa - 1)$ by $e_0, \dots, e_{\kappa-1}$, respectively (see Fig. 12), then the inflow penetrating into A_u^{cycle} is represented by

$$\rho_u = P_u [b_u \psi^{\text{BU}}(e_0), \dots, b_u \psi^{\text{BU}}(e_{\kappa-1})]^\top.$$

Recall that the arcs in the island u are denoted by $f_0, \dots, f_{\kappa-1}$ and the arcs from the outside of island u are denoted by $e_0, \dots, e_{\kappa-1}$. Then we have the following lemma.

Lemma 3. Let ψ^{BU} be a generalized eigenvector of U^{BU} satisfying $U^{\text{BU}} \psi^{\text{BU}} = \psi^{\text{BU}}$. Set

$$\begin{aligned} \varphi_{u,\text{in}} &= [\psi^{\text{BU}}(e_0), \dots, \psi^{\text{BU}}(e_{\kappa-1})]^\top, \\ \varphi_{u,\text{out}} &= [\psi^{\text{BU}}(\bar{e}_0), \dots, \psi^{\text{BU}}(\bar{e}_{\kappa-1})]^\top, \\ \varphi_{u,0} &= [\psi^{\text{BU}}(f_0), \dots, \psi^{\text{BU}}(f_{\kappa-1})]^\top. \end{aligned}$$

Then we have

$$\varphi_{u,\text{out}} = \text{Circ}(H_u) \varphi_{u,\text{in}}, \quad (17)$$

$$\varphi_{u,0} = \frac{1}{c_u} (\text{Circ}(H_u) - d_u I_u) \varphi_{u,\text{in}}. \quad (18)$$

Proof. It holds that

$$\begin{aligned} \varphi_{u,\text{out}}(j) &= c_u \varphi_{u,0}(j) + d_u \varphi_{u,\text{in}}(j) \\ &= c_u ((1 - E_u)^{-1} \rho_u)(j) + d_u \varphi_{u,\text{in}}(j) \\ &= c_u ((1 - E_u)^{-1} P_u b_u \varphi_{u,\text{in}})(j) + d_u \varphi_{u,\text{in}}(j). \end{aligned} \quad (19)$$

Then we have

$$\varphi_{u,\text{out}} = (b_u c_u (1 - E_u)^{-1} P_u + d_u) \varphi_{u,\text{in}}.$$

The inverse of $(1 - E_u)$ can be expressed by

$$\begin{aligned} (1 - E_u)^{-1} &= 1 + a_u P_u + (a_u P_u)^2 + \dots \\ &= 1 + (a_u + a_u^{\kappa+1} + a_u^{2\kappa+1}) P_u \\ &\quad + (a_u^2 + a_u^{\kappa+2} + a_u^{2\kappa+2} + \dots) P_u^2 \\ &\quad + \dots + (a_u^{\kappa-1} + a_u^{\kappa+\kappa-1} + a_u^{2\kappa+\kappa-1} + \dots) P_u^{\kappa-1} \\ &= 1 + \frac{a_u}{1 - a_u^\kappa} P_u + \frac{a_u^2}{1 - a_u^\kappa} P_u^2 + \dots + \frac{a_u^{\kappa-1}}{1 - a_u^\kappa} P_u^{\kappa-1}. \end{aligned}$$

Then inserting the above expression for $(1 - E)^{-1}$ into $b_u c_u (1 - E_u)^{-1}$, we obtain $\text{Circ}(H_u) = b_u c_u (1 - E_u)^{-1} P_u + d_u I_u$, which completes the proof of (17). We obtain (18) by combining (19) with (17). ■

Thus $\text{Circ}(H_u)$ represents the local scattering matrix of the n -directed cycle with n boundaries for the in- and outflow. The unitarity of $\text{Circ}(H_u)$ is ensured by Refs. [12,13] in more general settings.

Next, let us introduce the restriction $\iota : \mathbb{C}^{\tilde{A}_0^{\text{BU},\xi}} \rightarrow \mathbb{C}^{\tilde{A}_0}$ such that $(\iota \psi)(a) = \psi(a)$ for any $a \in \tilde{A}_0$. A matrix representation of ι is given by

$$\iota \cong [I_{\tilde{A}_0} | 0]$$

under the decomposition of $\tilde{A}_0^{\text{BU},\xi}$ into $\tilde{A}_0 \sqcup A_0^{\text{cycle}}$.

Then we have the following proposition.

Proposition 2. For any $\psi \in \mathbb{C}^{\tilde{A}_0^{\text{BU},\xi}}$ satisfying a generalized eigenequation $U^{\text{BU}} \psi = \psi$, we have

$$U_0 \iota \psi = \iota \psi.$$

Proof. By (17) in Lemma 3, we immediately obtain the conclusion. ■

We expect that $\iota \psi$ is the stationary state of the circulant QW, but unfortunately, it is not true in general. See Example 2 in Sec. V. So in the following, let us consider when $\iota \psi$ coincides with the stationary state of the circulant QW. To this end, we prepare the following two propositions.

Proposition 3. $\ker(1 - U_0) \neq \{\mathbf{0}\}$ if and only if $\ker(1 - U^{\text{BU}}) \neq \{\mathbf{0}\}$.

Proof. Assume $\ker(1 - U_0) \neq \{\mathbf{0}\}$, that is, there exists $\phi \neq \mathbf{0}$ such that $U_0 \phi = \phi$ and $\text{supp}(\phi) \subset A_0$. Let

$$\{e_0, \dots, e_{\kappa-1}\} = \{a \in \tilde{A}_0 \mid t(a) = u\}$$

and

$$\varphi_{u,\text{in}} = [\phi(e_0), \dots, \phi(e_{\kappa-1})]^\top.$$

Then let us define $\psi \in \mathbb{C}^{\tilde{A}_0^{\text{BU},\xi}}$ by

$$\psi(a) = \begin{cases} \phi(a) & : a \in \tilde{A}_0 \\ \frac{1}{c_u} ((\text{Circ}(H_u) - d_u I_u) \varphi_{u,\text{in}})(a) & : a \in A_{0,u}^{\text{cycle}}, u \in V_0. \end{cases} \quad (20)$$

By Lemma 3, we have $U^{\text{BU}}\psi = \psi$, and the support of ψ does not have the overlap with the tails, which implies that $\|\psi\| < \infty$. Next, let us consider the converse direction. Note that $\text{spec}(E_u) \subset \{z \in \mathbb{C} \mid |z| < 1\}$. Then the support of the eigenvectors of eigenvalue 1 must have the overlap to \tilde{A}_0 . Then, from Proposition 2, we obtain the converse direction. ■

Remark 3. Proposition 3 implies that the eigenvectors of $\ker(1 - U_0)$ have one-to-one correspondence to those of $\ker(1 - U^{\text{BU}})$.

Proposition 4. Assume $\ker(1 - U_0) = \{\mathbf{0}\}$. Then for arbitrary $s_0 \in \mathbb{C}^{\tilde{A}_+}$, the following generalized eigenfunction satisfying the boundary condition $\psi|_{\partial A_+} = s_0$ is uniquely determined:

$$(1 - U_0)\psi = 0, \quad \psi|_{\partial A_+} = s_0.$$

Proof. Let $\zeta : \mathbb{C}^{\tilde{A}_0} \rightarrow \mathbb{C}^{\tilde{A}_0 \setminus \text{tails}}$ such that $(\zeta\phi)(a) = \phi(a)$ for any $a \in \mathbb{C}^{\tilde{A}_0 \setminus \text{tails}}$. Putting $\zeta U_0 \zeta^* = E$, we have

$$(1 - E)\zeta\psi = \rho,$$

where $\rho = \zeta U_0(1 - \zeta^*\zeta)\psi$. Let us see that $(1 - E)^{-1}$ exists as follows. Assume there is a $f \neq 0$ such that $Ef = f$. Taking the operation ζ^* to both sides, we have $\|\zeta^*\zeta U_0 \zeta^* f\|^2 = \|\zeta^* f\|^2$. On the other hand, by the unitarity of U_0 , we have $\|U_0 \zeta^* f\|^2 = \|\zeta^* f\|^2$. Then we have $\|U_0 \zeta^* f\| = \|\zeta^* \zeta U_0 \zeta^* f\|$. Since $\zeta^* \zeta$ is a projection onto the internal graph, this implies that the support of $U_0 \zeta^* f$ is included in the internal graph; that is, $(1 - \zeta^* \zeta)U_0 \zeta^* f = 0$. This is equivalent to $U_0 \zeta^* f - \zeta^* E f = 0$. Since $Ef = f$, we have $(1 - U_0)\zeta^* f = 0$. Thus $\zeta^* f (\neq 0)$ is an $(+1)$ eigenvector of U_0 , which contradicts the assumption $\ker(1 - U_0) = \{\mathbf{0}\}$. Therefore we have $\zeta\psi = (1 - E)^{-1}\rho$, which implies that $\zeta^*\zeta\psi = \xi(1 - E)^{-1}\rho$. Thus the restriction of ψ to the internal graph is uniquely determined. On the other hand, the restriction of ψ to the tails is uniquely determined as s_0 for the inflow and $(1 - \zeta^* \zeta)U_0 \zeta^* \psi$ for the outflow. ■

Now we are ready for the proof of Proposition 1: If $\ker(1 - U^{\text{BU}}) = \{\mathbf{0}\}$, then $\text{Opt}(\text{QW}(G_0; \mathbf{H}; \xi))$ implements $\text{QW}(G_0; \mathbf{H}; \xi)$.

Proof of Proposition 1. Let Ψ be the stationary state of the optical QW. We set the boundary condition by $\Psi|_{\partial A_+} = s_0$. The assumption of Proposition 1 is equivalent to $\ker(1 - U_0) = \{\mathbf{0}\}$ by Proposition 3, which is the assumption of Proposition 4. Then by Proposition 4, the unique solution of $(1 - U_0)\psi = 0$ with $\psi|_{\partial A_+} = s_0$ is nothing but the stationary state of the circulant QW with the inflow represented by s_0 . On the other hand, by Proposition 2, we have $U_0 \iota \Psi = \iota \Psi$. In particular, $\iota \Psi|_{\partial A_+} = \Psi|_{\partial A_+} = s_0$. Therefore, the unique solution ψ is described by $\iota \Psi$, which implies that the stationary state for the circulant QW is equivalent to $\psi = \iota \Psi$. ■

Remark 4. In general, the stationary state of QWs must be orthogonal to every eigenspace of the time evolution operators in the whole space [14]. Let $\psi_\infty^{(\text{BU})}$ be the stationary state of the optical QW. Then for any $\phi \in \ker(1 - U^{(\text{BU}, \xi)})$, we have

$$\langle \psi_\infty^{(\text{BU})}, \phi \rangle = 0.$$

However, in general, it is not ensured that

$$\langle \iota \psi_\infty^{(\text{BU})}, \iota \phi \rangle = 0. \quad (21)$$

This is the reason that the optical QW does not implement the underlying QW in Example 2 since the optical QW has eigenvalue 1 and does not satisfy (21).

Remark 5. Conversely, if $\ker(1 - U_0) = \{\mathbf{0}\}$, then the stationary state ψ_∞ implements the stationary state of $\psi_\infty^{(\text{BU})}$ by the manner of deformation of ψ_∞ given by (20) in Proposition 3. This means that two stationary states on \tilde{G}_0 and $\tilde{G}^{(\text{BU}, \xi)}$ implement each other under the condition of $\ker(1 - U_0) = \{\mathbf{0}\}$.

IX. SUMMARY AND DISCUSSION

In this paper, we considered an optical implementation of QW on a graph driven by a circulant matrix, namely, the circulant QW. To this end, we introduced another kind of QW on the blow-up graph of the original graph induced by the circulant QW; this was the optical QW. The blow-up graph is a two-regular directed graph. Then making a correspondence between the two incoming edges to each vertex and the vertical and horizontal polarizations, we heuristically showed that the optical QW can be implemented by the optical circuit in theory and also proposed the design of the optical circuit for the general graph. We suggested a kind of search of a perturbed vertex using our circulant QW. A high relative probability of the perturbed vertex is asymptotically stable, while such a probability is asymptotically periodic in the usual quantum search algorithm driven by QWs. The analysis on this convergence speed has the potential to consider a QW version of the cutoff phenomena [2,3] in the future. We also mathematically showed a sufficient condition for the coincidence of the stationary states of the circulant QW and its induced optical QW. From this condition, we gave a useful setting for the circulant QW that can be implemented by the induced optical QW.

Finally, let us discuss the design of the optical circuit in Sec. IV, as an experimental approach to potential problem in the future. In Sec. IV, we designed the optical circuit under ideal conditions where the phases are matched, but experimentally the phases are not matched due to the noise arising from complex environmental fluctuation, so the expected operation does not occur in HWPs. To solve this problem, we propose an experimental method. In an optical circuit such as that in Sec. IV 1, it is necessary to make the optical path length of one round trip of V-polarized light be an integer multiple of the wavelength to obtain constructive interference with the light from previous laps. It is also necessary to match the phases of waves at each PBS. To meet these requirements, we stabilize the optical path length between each pair of PBSs. Experimentally, stabilization of the length of the optical circuit can be achieved by a feedback control by using a reference laser and a piezoelectric transducer which can be attached to a mirror consisting of the optical circuit [25]. If necessary, the phase of the incoming signal is also stabilized by a similar procedure. Also, in Sec. IV 2, each pair of islands is connected together following the original graph connection; the resulting design is described by G' . The ideal design G' is implemented with optical elements as shown on the right of

Fig. 4. The polarized light that flows out from G' does not return to G' , so there is no need to consider the optical path length. On the other hand, H-polarized light flowing out from one island to another interferes with V-polarized light at the PBS of the destination island, so the optical path length needs to be stabilized by the same feedback control. However, in the above method, we should measure the outflow from each PBS to perform feedback control in the optical path between each PBS. Then, a trade-off problem remains in that the more accurately we try to get the interference inside the island, the more we lose the output outside the island. We expect that such realistic experimental problems based on our proposed

optical circuit under very ideal conditions will be improved in the future.

ACKNOWLEDGMENTS

Yu.H. acknowledges financial support from the Grant-in-Aid of Scientific Research Japan Society for the Promotion of Science (Grant No. 18K03401). E.S. acknowledges financial support from the Grant-in-Aid of Scientific Research Japan Society for the Promotion of Science (Grant No. 19K03616) and Research Origin for Dressed Photon.

-
- [1] P. G. Doyle and J. L. Snell, *Random Walks and Electric Networks* (Mathematical Association of America, Washington, DC, 1984).
- [2] P. Diaconis, *Group Representations in Probability and Statistics*, Lecture Notes—Monograph, Series Vol. 11 (Institute of Mathematical Statistics, Hayward, CA, 1988).
- [3] D. A. Levin and Y. Peres, *Markov Chains and Mixing* (American Mathematical Society, Providence, 2017).
- [4] A. Ambainis, E. Back, A. Nayak, A. Vishwanath, and J. Watrous, One-dimensional quantum walks, in *Proceedings of the Thirty-third Annual ACM Symposium on Theory of Computing* (ACM Press, New York, 2001), pp. 60–69.
- [5] R. P. Feynman and A. R. Hibbs, emended ed., *Quantum Mechanics and Path Integrals* (Dover Publications, Mineola, NY, 2010).
- [6] A. Ambainis, Quantum walks and their algorithmic applications, *Int. J. Quantum Inform.* **1**, 507 (2003).
- [7] A. M. Childs, Universal Computation by Quantum Walk, *Phys. Rev. Lett.* **102**, 180501 (2009).
- [8] R. Portugal, *Quantum Walk and Search Algorithms*, 2nd ed. (Springer Nature, Switzerland, 2018).
- [9] G. Brassard, Searching a quantum phone book, *Science* **275**, 627 (1997).
- [10] L. K. Grover, Fixed-Point Quantum Search, *Phys. Rev. Lett.* **95**, 150501 (2005).
- [11] T. J. Yoder, G. H. Low, and I. L. Chuang, Fixed-Point Quantum Search with an Optimal Number of Queries, *Phys. Rev. Lett.* **113**, 210501 (2014).
- [12] E. Feldman and M. Hillery, Quantum walks on graphs and quantum scattering theory, in *Coding Theory and Quantum Computing*, edited by D. Evans, J. Holt, C. Jones, K. Klintonworth, B. Parshall, O. Pfister, and H. Ward, *Contemp. Math.* **381**, 71 (2005).
- [13] E. Feldman and M. Hillery, Modifying quantum walks: A scattering theory approach, *J. Phys. A: Math. Theor.* **40**, 11343 (2007).
- [14] Yu. Higuchi and E. Segawa, Dynamical system induced by quantum walks, *J. Phys. A: Math. Theor.* **52**, 395202 (2019).
- [15] Yu. Higuchi, M. Sabri, and E. Segawa, Electric circuit induced by quantum walks, *J. Stat. Phys.* **181**, 603 (2020).
- [16] Z. Zhao, J. Du, H. Li, T. Yang, Z.-B. Chen, and J.-W. Pan, Implement quantum random walks with linear optics elements, [arXiv:quant-ph/0212149](https://arxiv.org/abs/quant-ph/0212149).
- [17] A. Schreiber, K. N. Cassemiro, V. Potoček, A. Gábris, P. J. Mosley, E. Andersson, I. Jex, and Ch. Silberhorn, Photons Walking the Line: A Quantum Walk with Adjustable Coin Operations, *Phys. Rev. Lett.* **104**, 050502 (2010).
- [18] K. Manouchehri and J. Wang, *Physical Implementation of Quantum Walks* (Springer, Berlin, Heidelberg, 2014).
- [19] X. Qiang, T. Loke, A. Montanaro, K. Aungskunsiri, X. Zhou, J. L. O'Brien, J. B. Wang, and J. C. F. Matthews, Efficient quantum walk on a quantum processor, *Nat. Commun.* **7**, 11511 (2016).
- [20] K. Matsue, L. Matsuoka, O. Ogurisu, and E. Segawa, Resonant-tunneling in discrete-time quantum walk, *Studies: Math. Found.* **6**, 35 (2018).
- [21] S. Albeverio, F. Gesztesy, R. Høegh-Krohn, H. Holden, and P. Exner, *Solvable Model in Quantum Mechanics* (AMS Chelsea Publishing, Rhode Island, 2004).
- [22] H. Morioka, Generalized eigenfunctions and scattering matrices for position-dependent quantum walks, *Rev. Math. Phys.* **31**, 1950019 (2019).
- [23] P. J. Davis, *Circulant Matrices*, 2nd ed. (Chelsea, New York, 1994).
- [24] R. Simon and N. Mukunda, Minimal three-component SU(2) gadget for polarization optics, *Phys. Lett. A* **143**, 165 (1990).
- [25] H.-A. Bachor and T. C. Ralph, *A Guide to Experiments in Quantum Optics* (Wiley-VCH, Weinheim, Germany, 2004).